Herschel far-infrared surveys of nearby galaxy clusters

Jon Davies and the HeViCS team

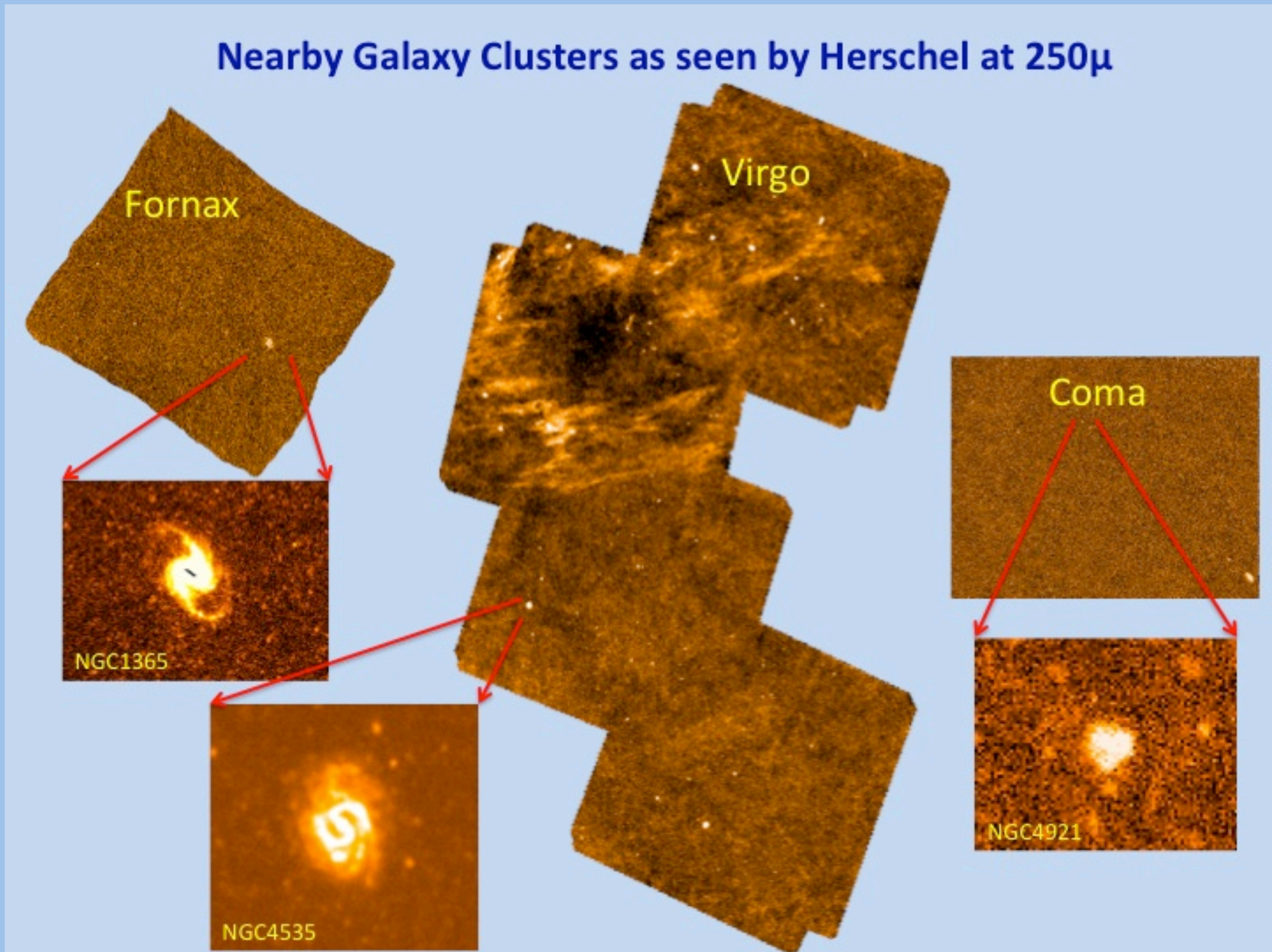

Scan maps at:
100μm
160μm
250μm
350μm
500μm

HeViCS consortium Members

Davies, J. I.; Baes, M.; Bendo, G. J.; Bianchi, S.; Bomans, D. J.; Boselli, A.; Clemens, M.; Corbelli, E.; Cortese, L.; Dariush, A.; de Looze, I.; di Serego Alighieri, S.; Fadda, D.; Fritz, J.; Garcia-Appadoo, D. A.; Gavazzi, G.; Giovanardi, C.; Grossi, M.; Hughes, T. M.; Hunt, L. K.; Jones, A. P.; Madden, S.; Pierini, D.; Pohlen, M.; Sabatini, S.; Smith, M. W. L.; Verstappen, J.; Vlahakis, C.; Xilouris, E. M.; Zibetti, S.

HeViCS papers

I. Davies et al. (2010), 'The Central Virgo field'
II. Cortese et al. (2010), 'Truncated dust discs'
III. Clemens et al. (2010), 'Dust lifetimes in early type galaxies'
IV. Smith et al. (2010), 'Dust surface density and temperatures'
V. Grossi et al. (2010), 'Metal poor star forming dwarfs'
VI. Baes et al. (2010), 'FIR emission from M87'
VII. de Looze et al. (2010), 'FIR emission from dwarf elliptical'
VIII. Davies et al. (2012), 'The Bright galaxy sample'
IX. Magrini et al. (2011), 'Dust-to-gas ratios and metalicity gradients'
X. Corbelli et al. (2012), 'The cold dust molecular gas relation'
XI. Papalardo et al. (2012), 'Environmental effects on molecular gas and dust'
XII. Auld et al. (2013), 'FIR observations of 251 Virgo cluster galaxies'
XIII. di Serego et al. (2013), 'Dust properties of early type galaxies'
XIV. de Looze et al. (2013), 'Transition dwarf galaxies'
XV. Baes et al. (2013), 'Compact Planck sources in HeViCS'
XVI. Davies et al. (2013), 'A cluster inventory'

HeFoCS papers

I. Davies et al. (2013), 'The bright galaxy sample'
II. Fuller et al. (2013), 'FIR observations of 30 Fornax cluster galaxies'

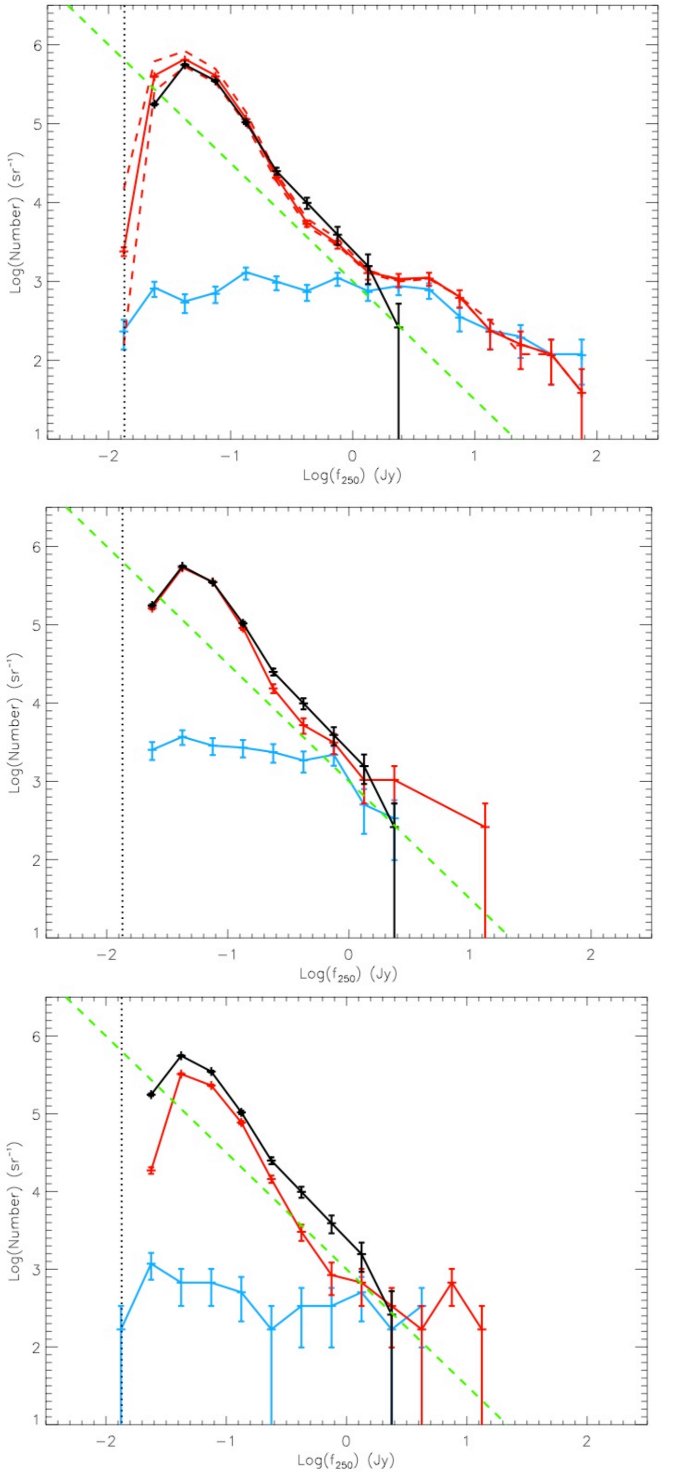

Davies et al. 2013

Virgo
251 galaxies
18 Mpc

Galaxy number counts
(250μ)

Coma
113 galaxies
96 Mpc

The rest of the talk will be about work
we are doing on the Virgo cluster

Fornax
30 galaxies
18 Mpc

Davies et al. 2013

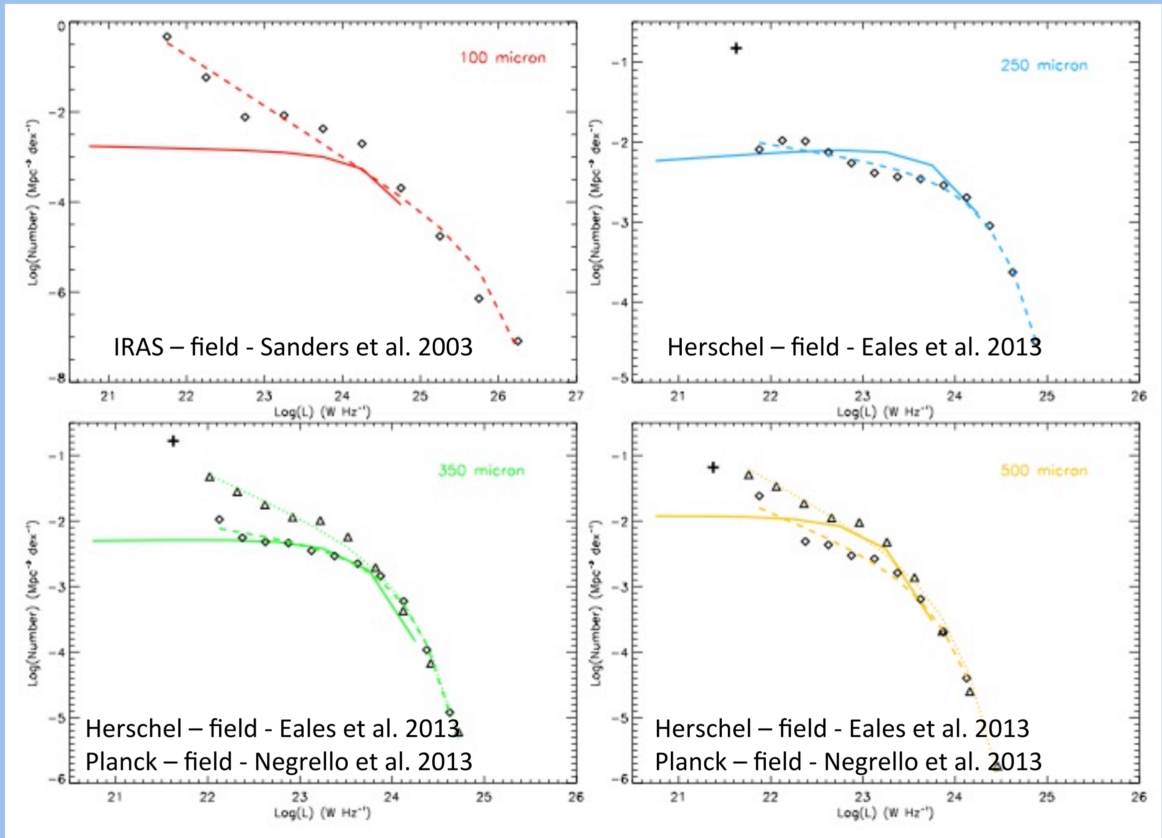

Virgo luminosity functions compared to the field

Band (μm)	Instrument	Region	α	L^* (10^{24} W Hz^{-1})	ϕ (Mpc^{-3} dex^{-1})	ρ_{FIR} (10^{23} W Hz^{-1} Mpc^{-3})
100	Herschel	Virgo	-1.0 ± 0.1	2.1 ± 0.6	0.3 ± 0.1	3.3
160	Herschel	Virgo	-1.0 ± 0.1	2.8 ± 1.0	0.3 ± 0.1	4.5
250	Herschel	Virgo	-0.9 ± 0.1	0.8 ± 0.2	0.6 ± 0.1	2.2
350	Herschel	Virgo	-1.0 ± 0.1	0.5 ± 0.1	0.5 ± 0.1	1.2
500	Herschel	Virgo	-1.0 ± 0.1	0.2 ± 0.01	0.5 ± 0.1	0.4
100	IRAS	Field	-2.1 ± 0.1	46 ± 15	0.000012 ± 0.000007	-
250	Herschel	Field	-1.19 ± 0.04	1.6 ± 0.1	0.0017 ± 0.0002	0.03
350	Herschel	Field	-1.22 ± 0.05	0.7 ± 0.1	0.0014 ± 0.0002	0.01
500	Herschel	Field	-1.58 ± 0.12	0.4 ± 0.1	0.0067 ± 0.0003	0.01
350	Planck	Field	-1.65 ± 0.08	0.9 ± 0.1	0.0013 ± 0.0003	0.03
550	Planck	Field	-1.78 ± 0.1	0.4 ± 0.1	0.0010 ± 0.0003	0.02

Cortese et al. 2010

Truncated dust disks in H I-deficient spirals

We show for the first time that the extent of the dust disk is significantly reduced in HI-deficient galaxies, following remarkably well the observed “truncation” of the HI disk. The cluster environment is able to strip dust as well as gas.

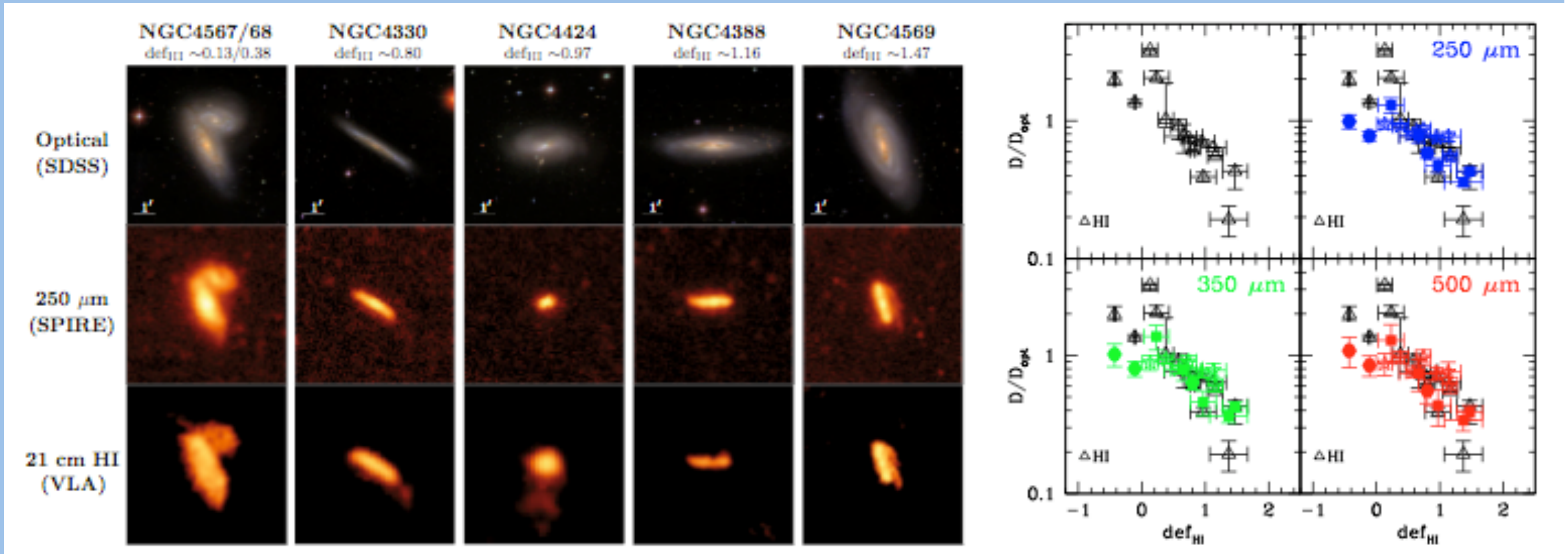

$def_{HI} = \langle \log M_{HI}(D,T) \rangle - \log M_{HI}(D,T)_{obs}$

de Looze et al. 2013

Dust in cluster dwarf elliptical galaxies

The first far-infrared detection of cluster early-type dwarf galaxies – transition types

Dust scaling relations support the hypothesis of a transformation between infalling late- type galaxies to quiescent low-mass spheroids governed by environmental effects, with dust- to-stellar mass fractions for transition-type dwarfs in between values characteristic for late- type objects and the lower dust fractions observed in early-type galaxies.

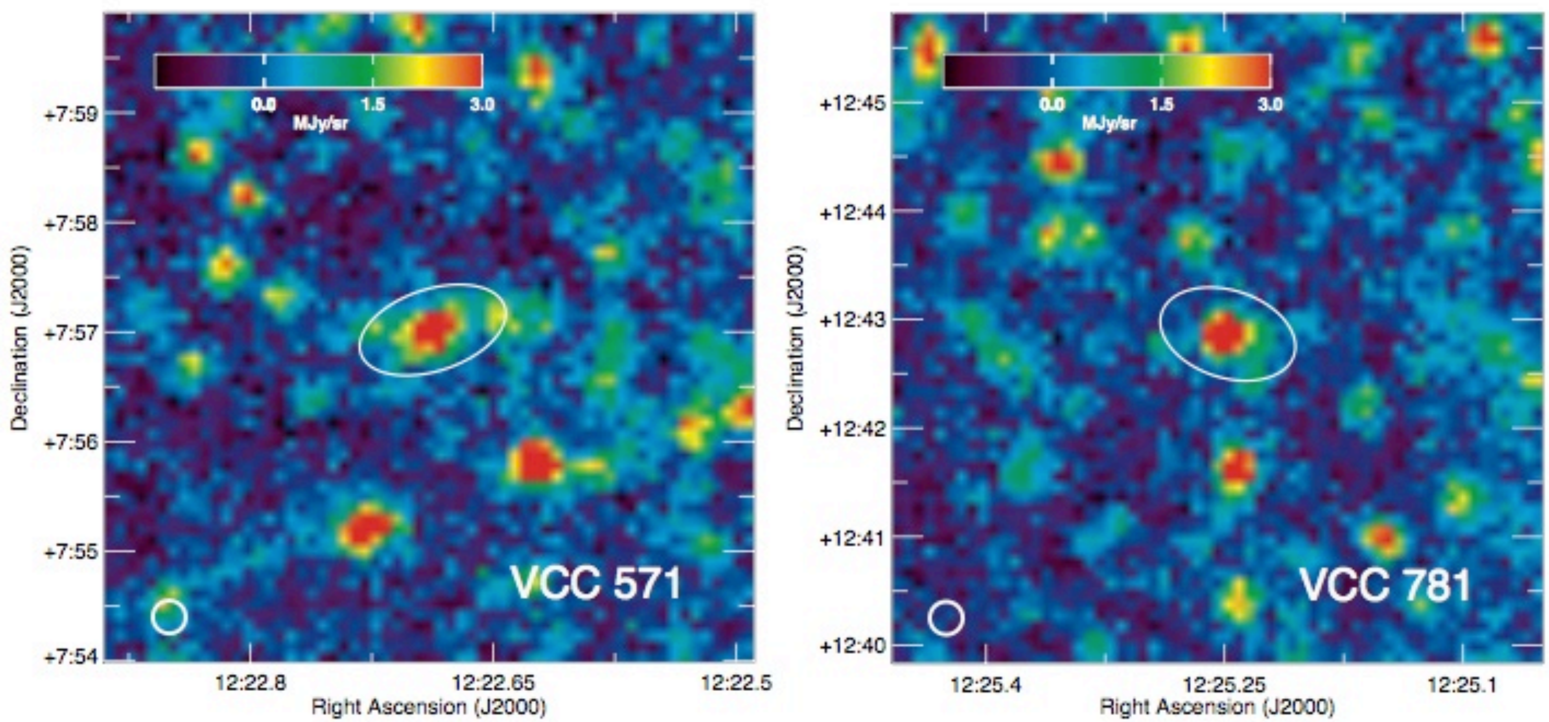

Figure 3. *Herschel* maps of the SPIRE 250 μm waveband for transition-type dwarfs, VCC 571 and VCC 781. The white ellipses correspond to the optical isophotal diameter D_{25} (25 mag arcsec^{-2}), convolved with the SPIRE beam at 250 μm. The size of the beam at SPIRE 250 μm is indicated in the lower left corner of each panel.

Davies et al. 2012

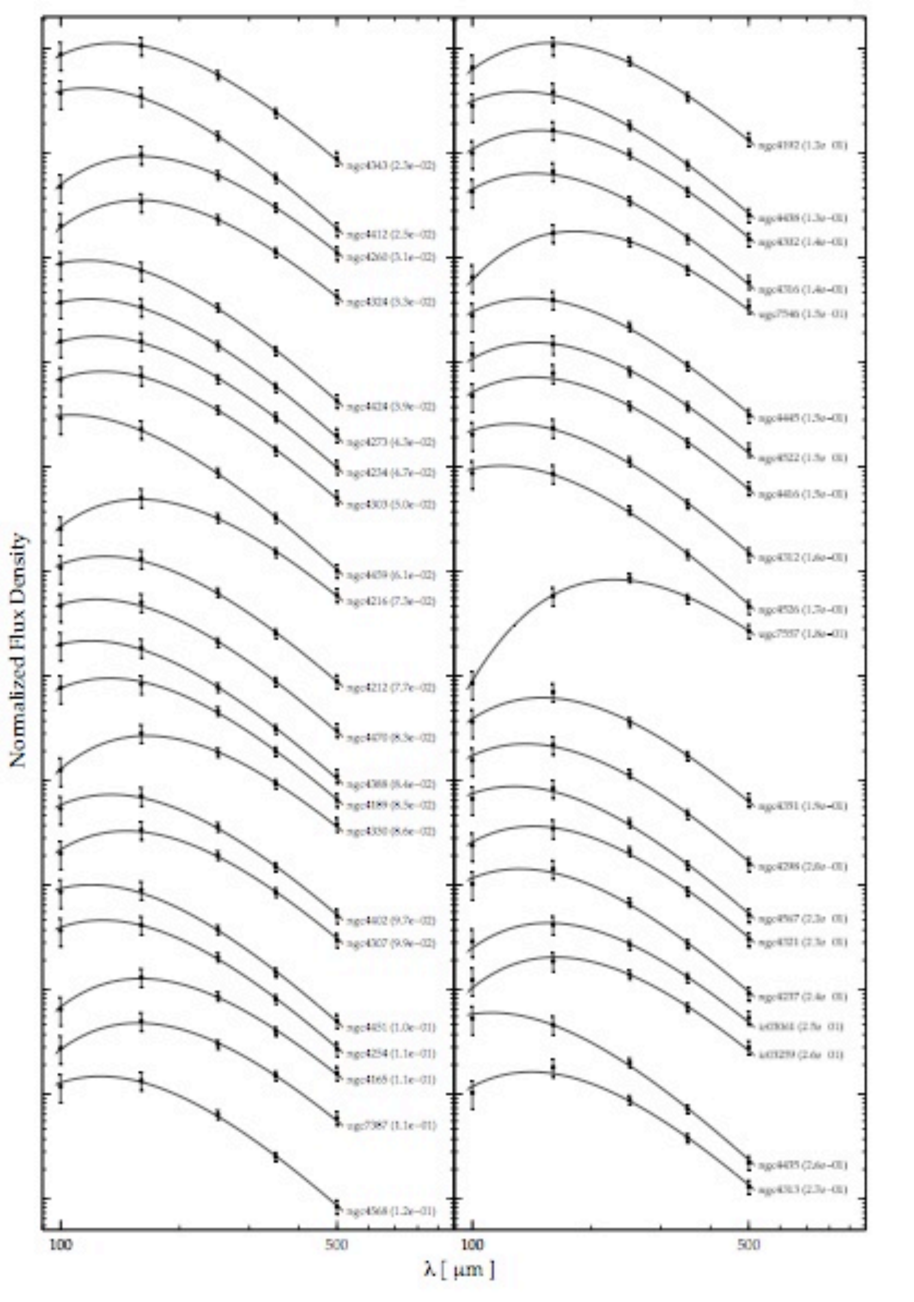

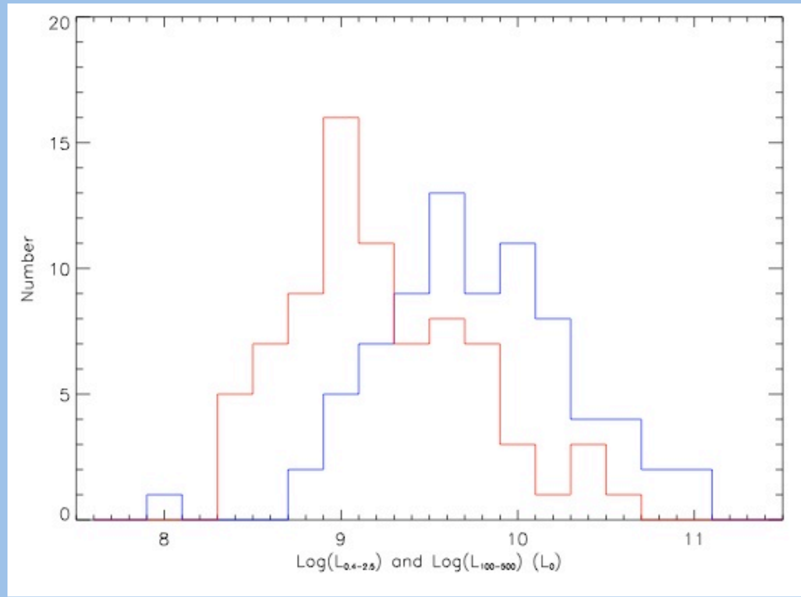

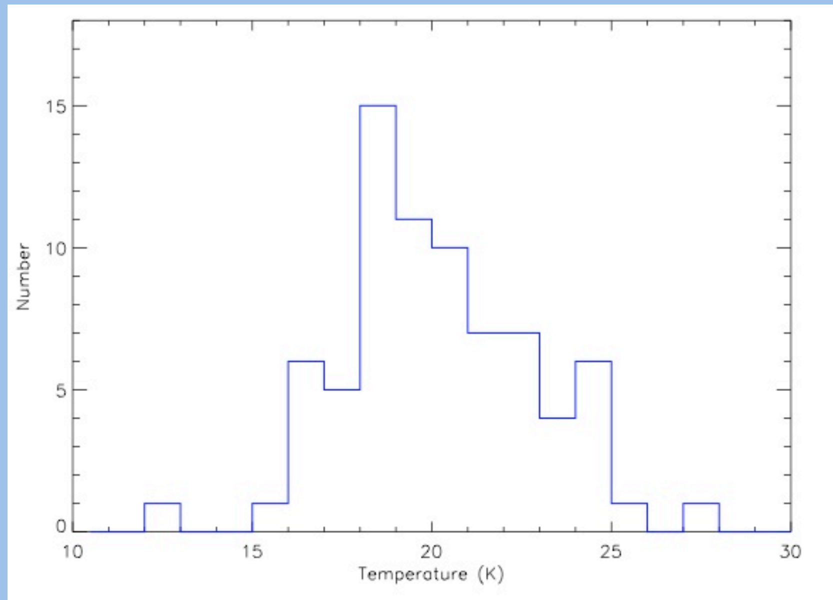

Spectral energy distributions

Davies et al. 2013

Dust properties

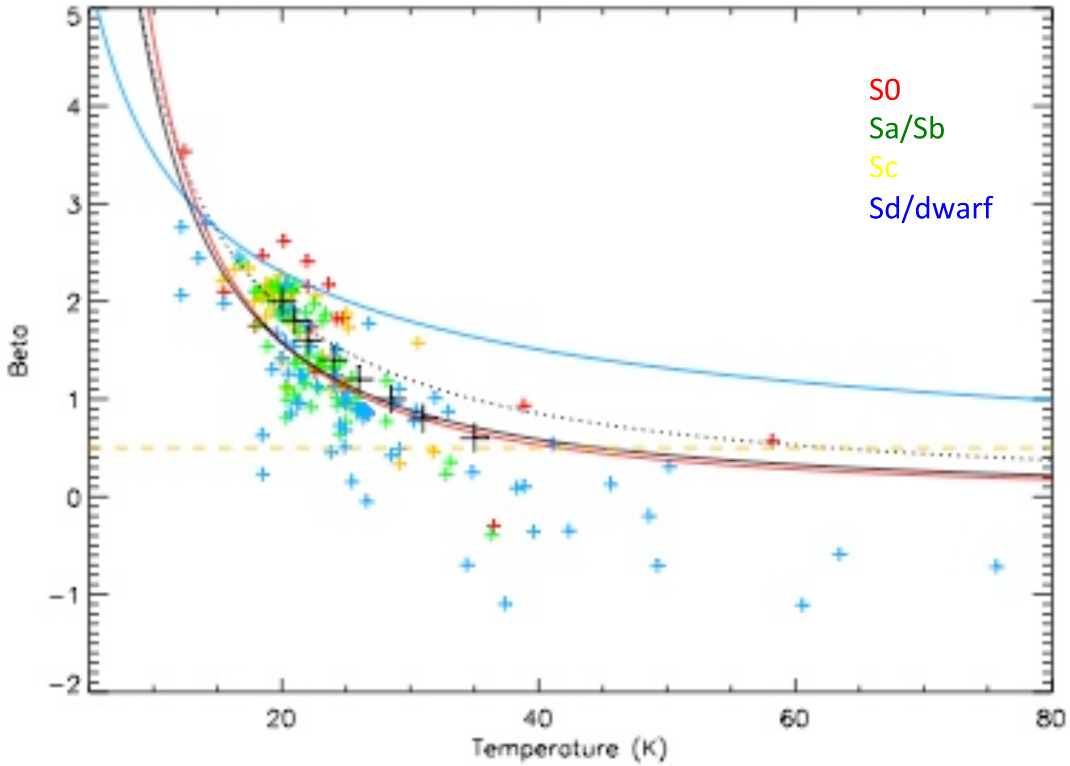

Figure 8. The relationship between dust temperature and dust emissivity index for 193 Virgo cluster galaxies. Galaxies are distinguished by their morphological type - earlier than Sa (red), Sa/Sb (yellow), Sc (green) and later than Sc (dwarfs and blue compact dwarfs) (blue). The solid black line is the best fitting line to the model described in the text using 146 galaxies later than S0. The black dotted line is the best fitting line to the model described in the text using 19 galaxies earlier than Sa (red points). The blue line is the relationship derived for regions within $R = 3.1$ kpc and the red line for $R > 3.1$ kpc as measured for M31 by Smith et al. (2012). The dashed yellow line indicates a value of $\beta = 0.5$. The large black crosses indicate the $\beta - T$ relation derived for local field galaxies by Clemens et al. (2013).

Smith et al. 2010

Resolved dust analysis of spiral galaxies

Herschel has unprecedented spatial resolution at far-infrared wavelengths and with the PACS and SPIRE instruments samples both sides of the peak in the far infrared spectral energy distribution. We can make maps of dust temperature, dust mass, emissivity index, gas-to-dust ratio and combine with a wealth of data at other wavelengths. These are produced by fitting modified black bodies to the SED for each pixel.

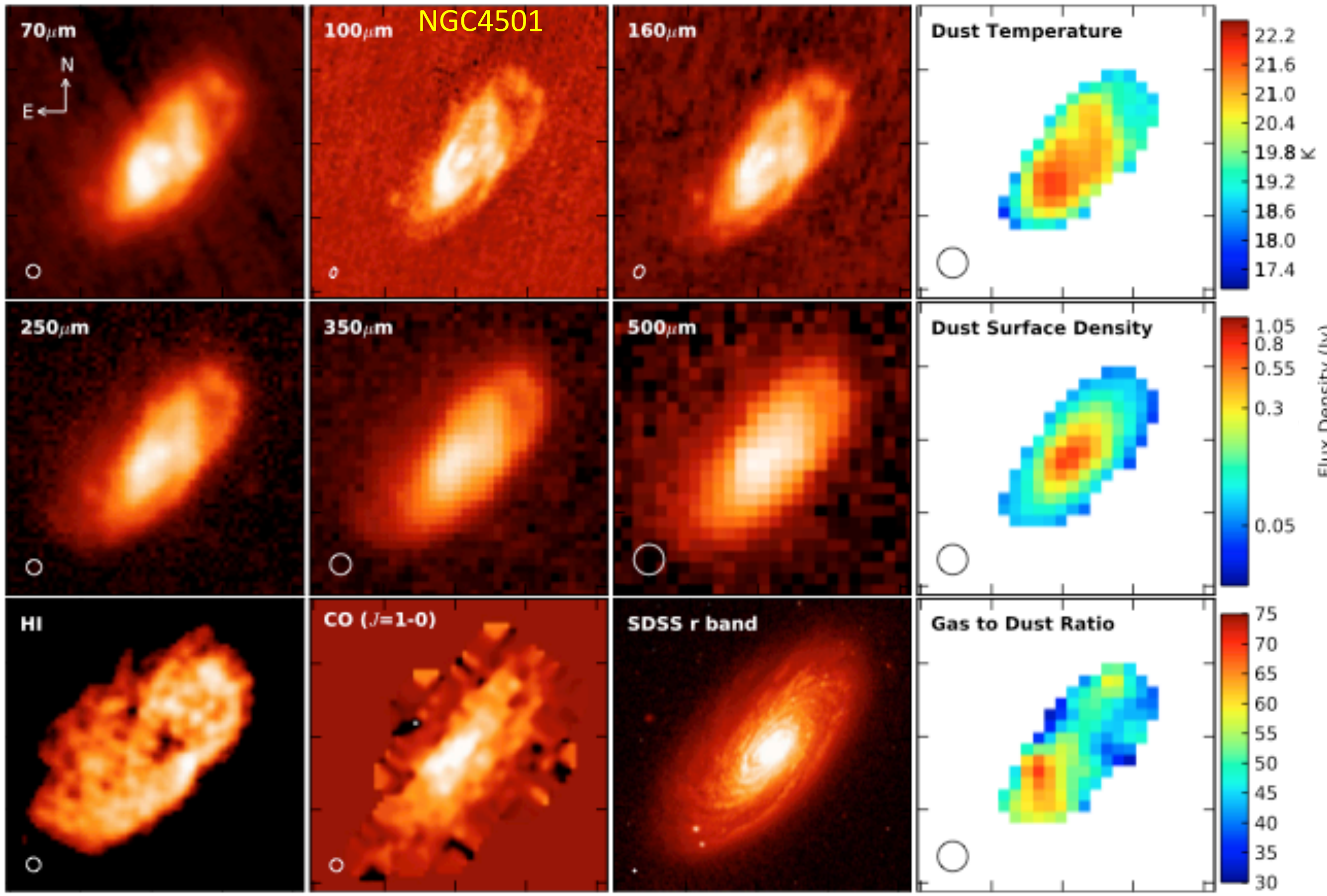

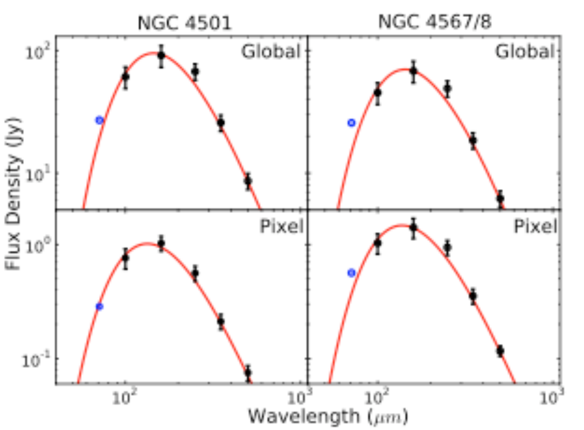

Grossi et al. 2010

Star-forming dwarf galaxies – dust in metal-poor environments

The dust properties of three Virgo cluster star forming dwarf galaxies.
These galaxies have low metallicities ($7.8 < 12 + \log(O/H) < 8.3$) and star-formation rates $\lesssim 10^{-1}\ M_\odot\ yr^{-1}$. We measure the spectral energy distribution (SED) from 100 to 500µm and derive dust temperatures and dust masses. The SEDs are fitted by a cool component of temperature $T \lesssim 20$ K, implying dust masses around $10^5\ M_\odot$ and dust-to-gas ratios within the range 10^{-3}-10^{-2}.

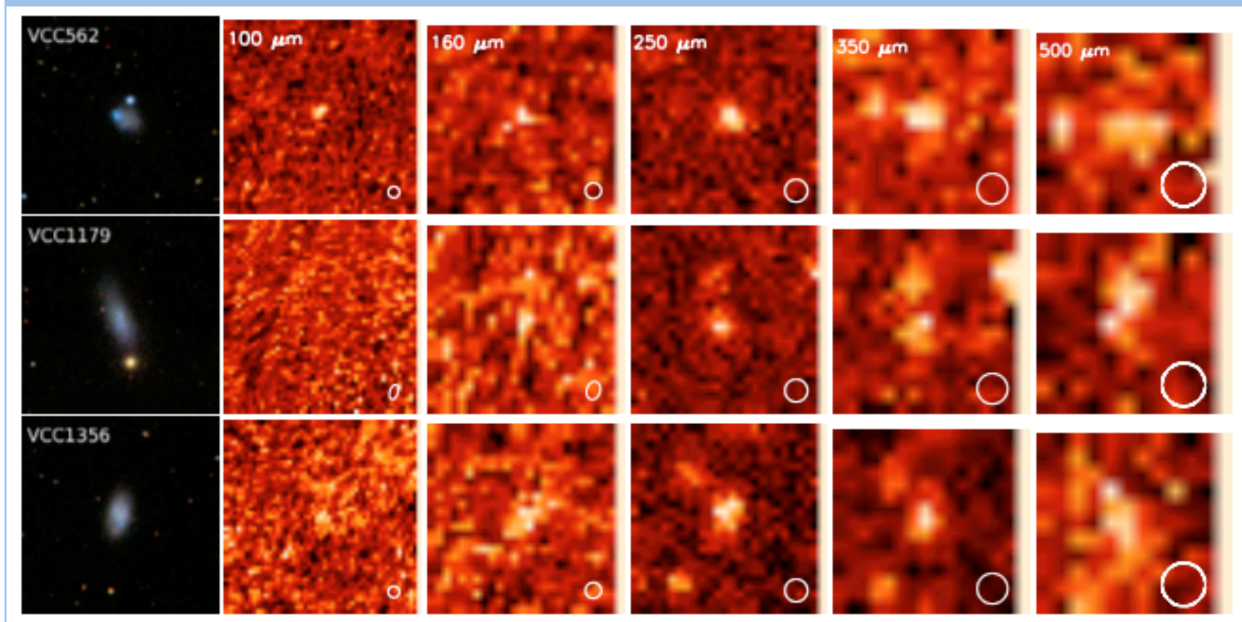

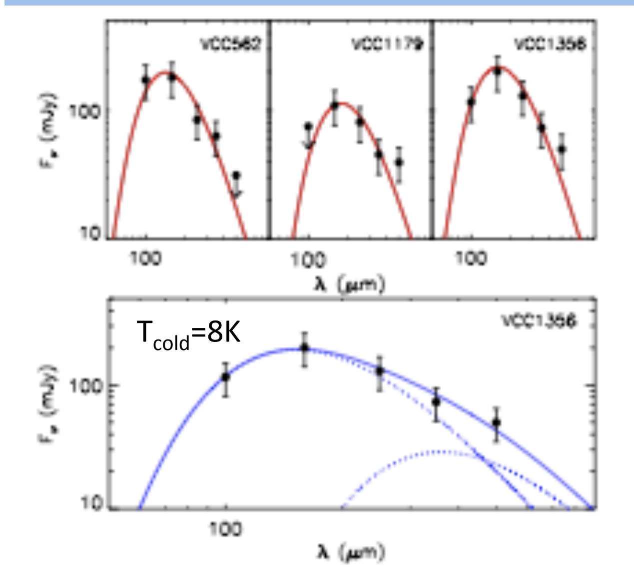

Baes et al. 2010

The far-infrared view of M 87

We compare Herschel data with a synchrotron model based on mid-infrared, far-infrared, sub-mm and radio data to investigate the origin of the far-infrared emission. Both the integrated SED and the Herschel surface brightness maps are adequately explained by synchrotron emission. At odds with previous claims, we find no evidence of a diffuse dust component in M 87.

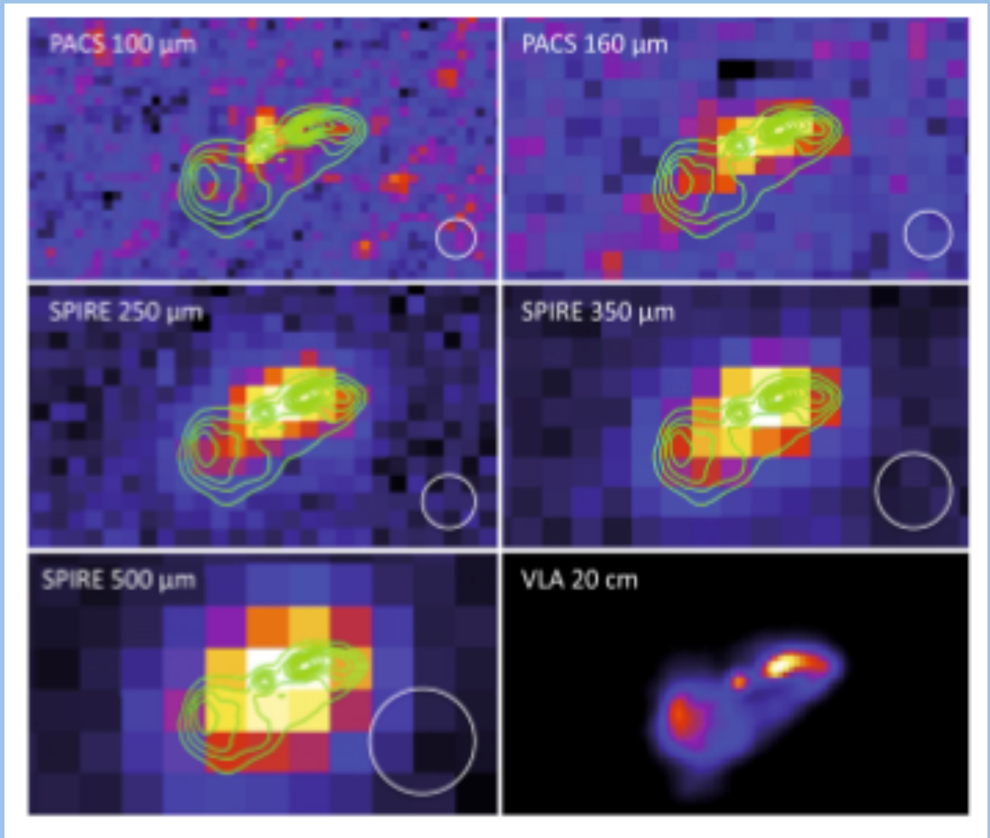

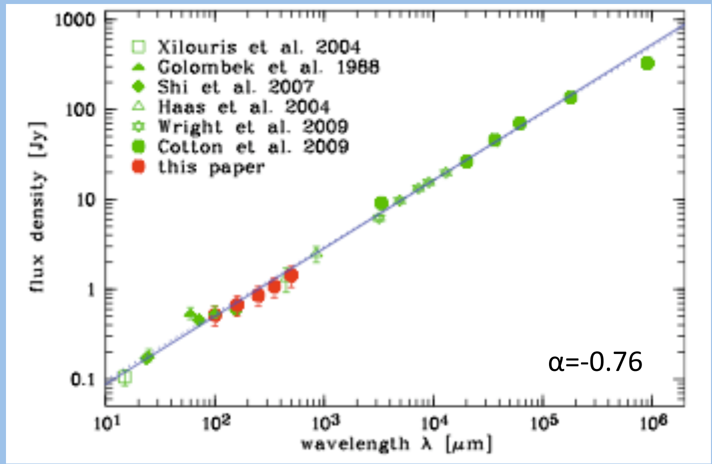

Davies et al. 2013

Baryonic mass Functions

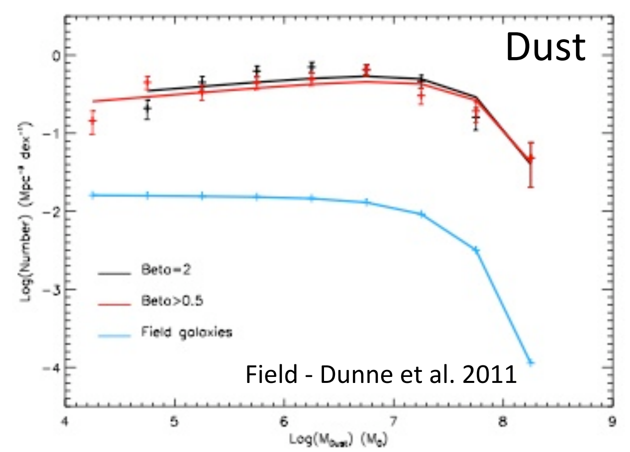

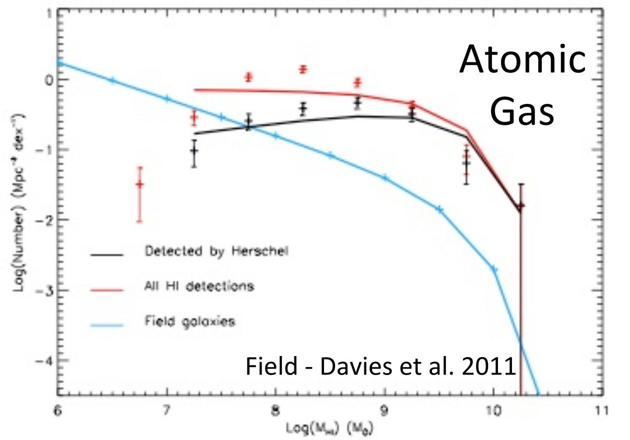

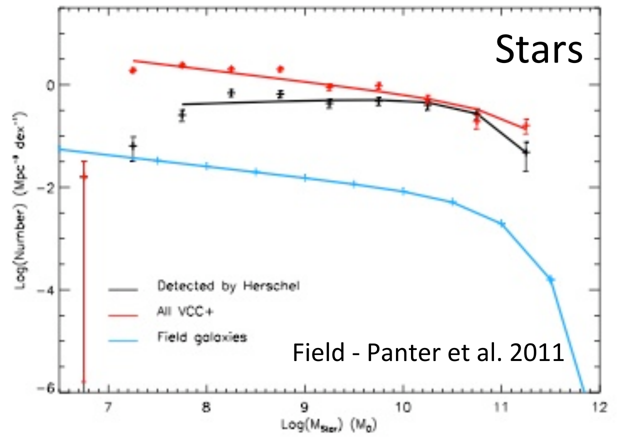

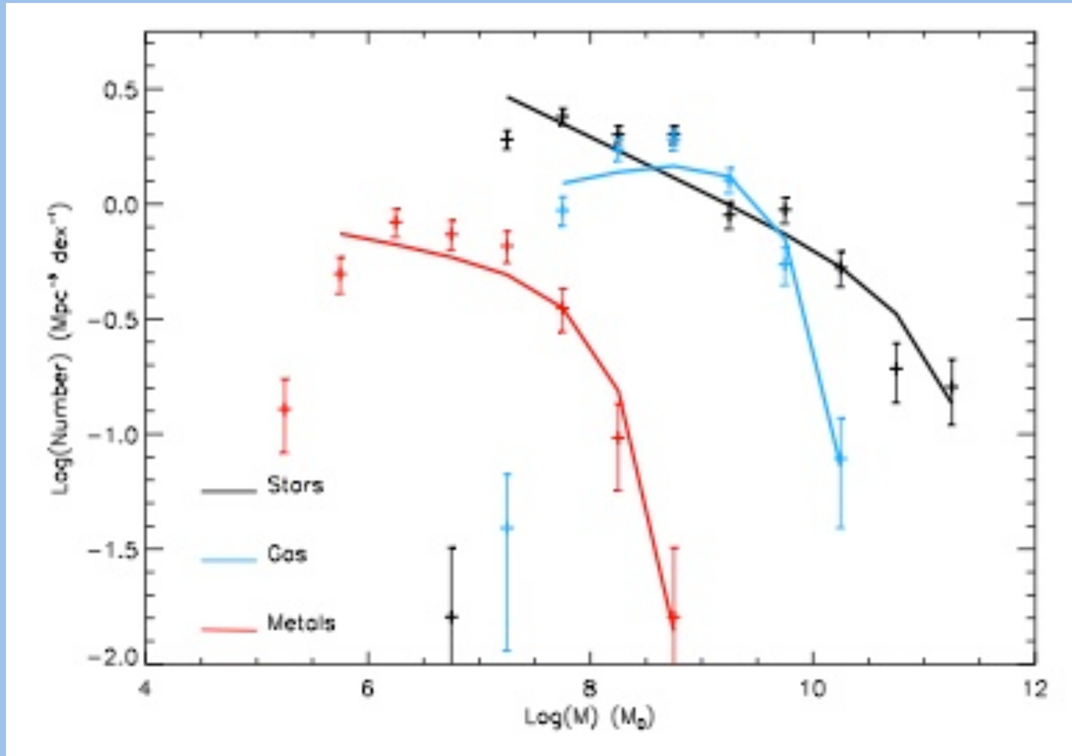

1. Molecular gas.
   Use $M_{H2} \propto M_{Dust}$
2. Helium. Use $M_{He}=M_{HI}/3.0$
3. Warm/Hot gas.
   Use $M_{WH}=M_{HI}$
4. Use mass metalicity relation (Hughes et al. 2013)

Baryonic Component	α	M^* ($M_\odot$)	ϕ (Mpc^{-3} dex^{-1})	ρ ($M_\odot$ Mpc^{-3})
Total stars	-1.2 ± 0.1	$1.9 \pm 1.2 \times 10^{11}$	0.3 ± 0.1	3.3×10^{10}
Total gas	-0.9 ± 0.1	$5.0 \pm 0.8 \times 10^{9}$	1.8 ± 0.3	4.3×10^{9}
Total metals	-1.1 ± 0.1	$1.7 \pm 0.3 \times 10^{8}$	0.4 ± 0.1	3.3×10^{7}

Find ratio of metals in the gas to that in the dust (50:50).

.

Davies et al. 2013

Chemical evolution

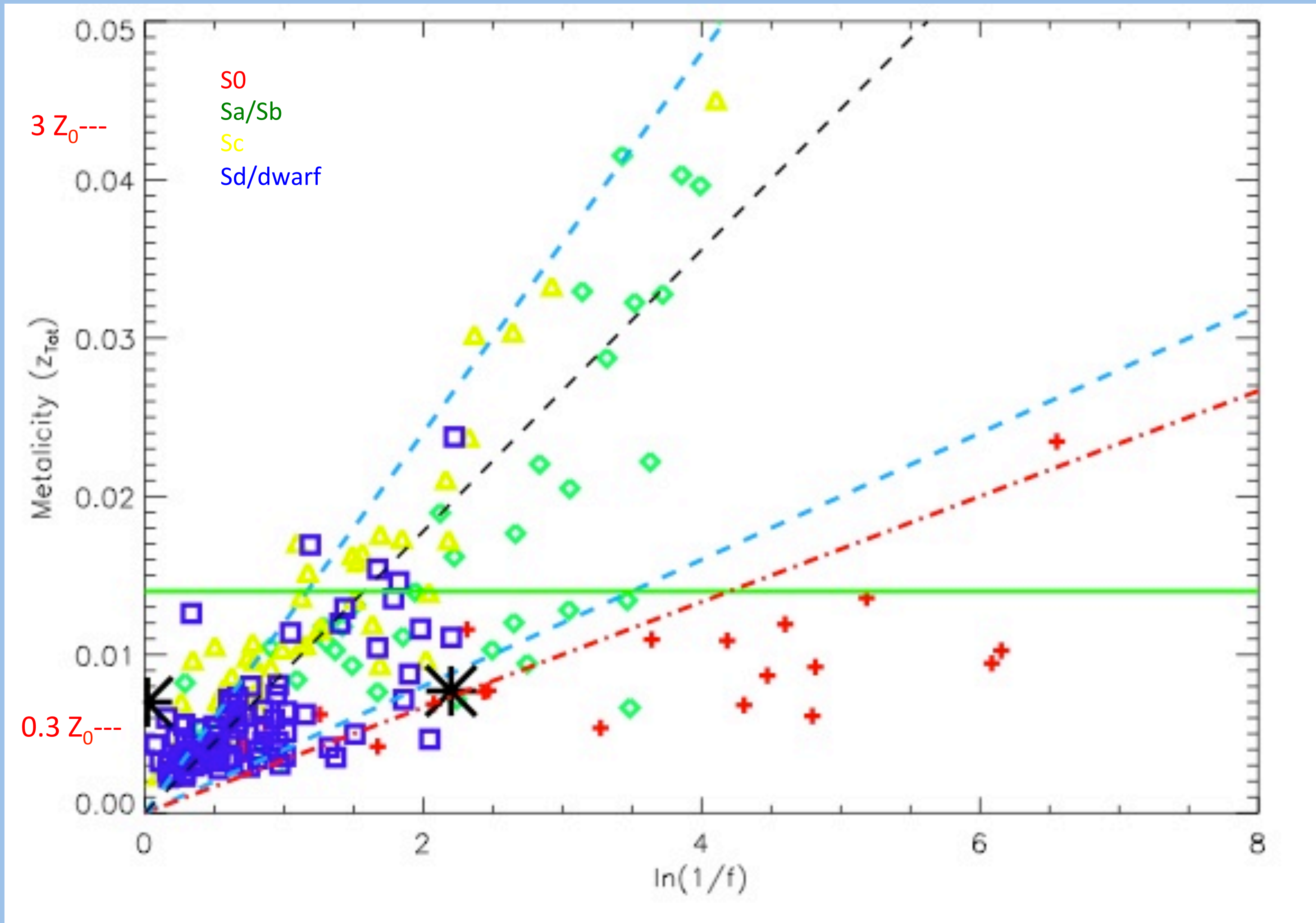

Davies et al. 2013

Star formation

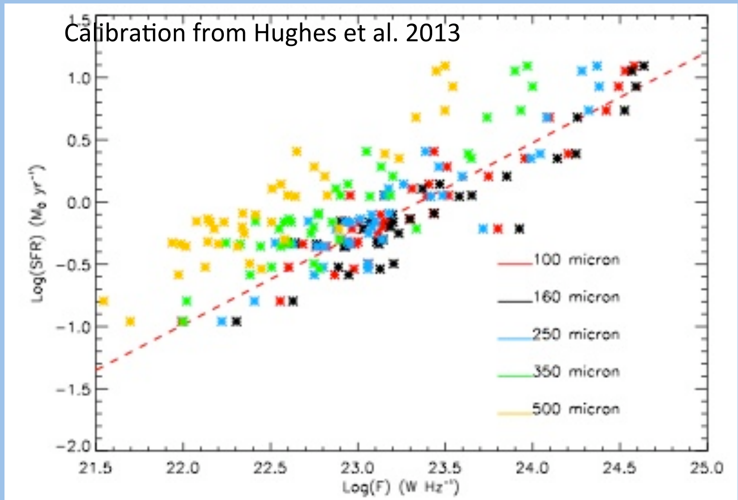

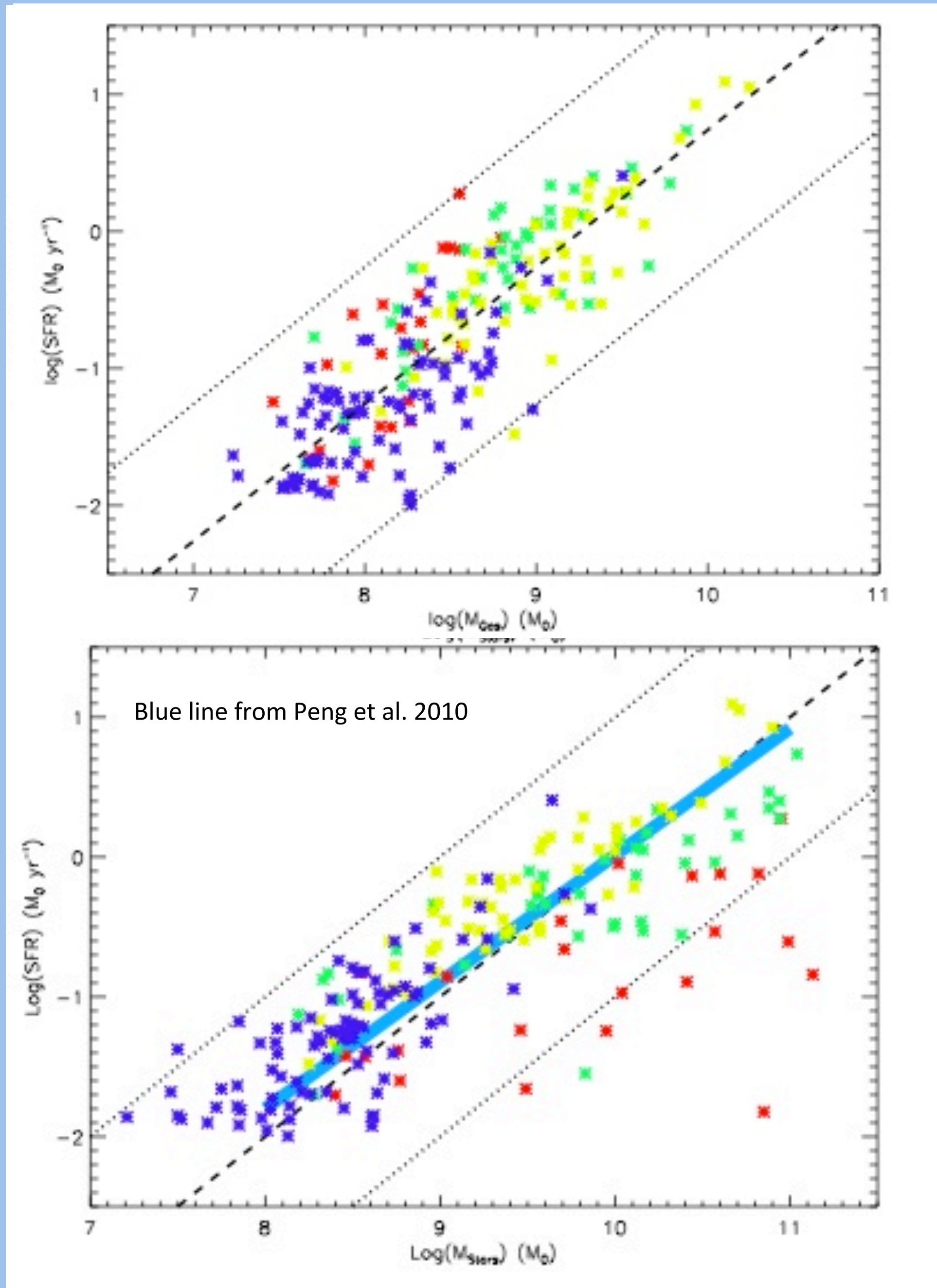

Summary

1. The Herschel Space Telescope has provided us with a unique opportunity to study the FIR properties of large numbers of large angular sized galaxies in nearby clusters. The proximity of these clusters also enables us to study large numbers of low mass systems.
2. No evidence for an additional faint FIR population in clusters not already identified by optical surveys.
3. Can fit FIR SEDs to get dust mass, temperature and an emissivity index.
4. Flat luminosity functions compared to the field (evolution in the cluster).
5. Dust discs truncated compared to the field (environmental effects).
6. Can derive dust mass, temperature, emissivity and gas-to-dust surface density maps.
7. Detect both star forming and passive dwarfs – FIR excess at long wavelengths.
8. Can combine Herschel data with other data to get:
   a) Chemical evolution.
   b) Star formation rate mass relation.
   c) Mass metalicity relation.
   d) Baryonic (stars, gas, metals) mass functions and mass densities.

All reduced data products from both HeViCS and HeFoCS are available